Review of Scientific Instruments

Development of a high resolution x-ray spectrometer for the National Ignition Facility (NIF)

Cite as: Rev. Sci. Instrum. **87**, 11E344 (2016); https://doi.org/10.1063/1.4962053
Submitted: 06 June 2016 . Accepted: 11 August 2016 . Published Online: 14 November 2016

K. W. Hill, M. Bitter, L. Delgado-Aparicio, P. C. Efthimion, R. Ellis, L. Gao, J. Maddox, N. A. Pablant, M. B. Schneider, H. Chen, S. Ayers, R. L. Kauffman, A. G. MacPhee, P. Beiersdorfer, R. Bettencourt, T. Ma, R. C. Nora, H. A. Scott, D. B. Thorn, J. D. Kilkenny, D. Nelson, M. Shoup, and Y. Maron

View Online Export Citation CrossMark

ARTICLES YOU MAY BE INTERESTED IN

A multi-cone x-ray imaging Bragg crystal spectrometer
Review of Scientific Instruments **87**, 11E333 (2016); https://doi.org/10.1063/1.4960537

Spatial resolution of a spherical x-ray crystal spectrometer at various magnifications
Review of Scientific Instruments **87**, 11D611 (2016); https://doi.org/10.1063/1.4960066

Calibration and characterization of a highly efficient spectrometer in von Hamos geometry for 7-10 keV x-rays
Review of Scientific Instruments **88**, 043110 (2017); https://doi.org/10.1063/1.4981793

MCL MAD CITY LABS INC. www.madcitylabs.com
Nanopositioning Systems
Modular Motion Control
AFM and NSOM Instruments
Single Molecule Microscopes

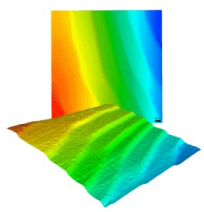
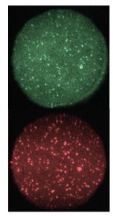

© 2016 Author(s).

AIP Publishing

Development of a high resolution x-ray spectrometer for the National Ignition Facility (NIF)

K. W. Hill,[1,a)] M. Bitter,[1] L. Delgado-Aparicio,[1] P. C. Efthimion,[1] R. Ellis,[1] L. Gao,[1] J. Maddox,[1] N. A. Pablant,[1] M. B. Schneider,[2] H. Chen,[2] S. Ayers,[2] R. L. Kauffman,[2] A. G. MacPhee,[2] P. Beiersdorfer,[2] R. Bettencourt,[2] T. Ma,[2] R. C. Nora,[2] H. A. Scott,[2] D. B. Thorn,[2] J. D. Kilkenny,[3] D. Nelson,[4] M. Shoup III,[4] and Y. Maron[5]
[1]*Princeton Plasma Physics Laboratory, Princeton, New Jersey 08543, USA*
[2]*Lawrence Livermore National Laboratory, Livermore, California 94551, USA*
[3]*General Atomics, San Diego, California 92121, USA*
[4]*Laboratory for Laser Energetics, University of Rochester, Rochester, New York 14623, USA*
[5]*Weizmann Institute of Science, Rehovot 76100, Israel*

(Presented 8 June 2016; received 6 June 2016; accepted 11 August 2016; published online 28 September 2016)

A high resolution (E/ΔE = 1200-1800) Bragg crystal x-ray spectrometer is being developed to measure plasma parameters in National Ignition Facility experiments. The instrument will be a diagnostic instrument manipulator positioned cassette designed mainly to infer electron density in compressed capsules from Stark broadening of the helium-β ($1s^2$-1s3p) lines of krypton and electron temperature from the relative intensities of dielectronic satellites. Two conically shaped crystals will diffract and focus (1) the Kr Heβ complex and (2) the Heα ($1s^2$-1s2p) and Lyα (1s-2p) complexes onto a streak camera photocathode for time resolved measurement, and a third cylindrical or conical crystal will focus the full Heα to Heβ spectral range onto an image plate to provide a time integrated calibration spectrum. Calculations of source x-ray intensity, spectrometer throughput, and spectral resolution are presented. Details of the conical-crystal focusing properties as well as the status of the instrumental design are also presented. *Published by AIP Publishing.* [http://dx.doi.org/10.1063/1.4962053]

I. INTRODUCTION

X-ray spectroscopy will be used in indirect drive experiments at the National Ignition Facility (NIF) to diagnose plasma conditions and mix in ignition capsules near stagnation times, thus indicating the quality of the implosion, and at various positions in the hohlraum. The electron temperature, T_e, and density, n_e, will be measured from dielectronic satellites and Stark broadening, respectively, by doping a surrogate capsule ("SymCap") with a small amount of Kr gas. These measurements will corroborate neutron based measurement of ion temperature, T_{ion}, assuming $T_e = T_{ion}$ due to quick equilibration at stagnation. This direct measurement of n_e will corroborate the inference of density from other measurements (T_{ion}, neutron yield, size of hotspot, and duration of burn). The T_e measurement in Kr doped capsules will also benchmark other measurements from the x-ray continuum slope, which will then measure T_e in igniting capsules (without Kr). Mixing of capsule ablator material and fill tube material into the fuel quickly degrades performance. X-ray spectroscopy of doped elements in the ablator will diagnose the amount of mix into the hot spot, and other effects of mix. In the hohlraum, x-ray spectroscopy will measure plasma conditions in the hot plasma where laser energy is deposited, giving insight into the underlying physics that govern hohlraum behavior and processes that directly affect x-ray drive, symmetry, and laser-hohlraum coupling.

The spectral ranges to be measured are illustrated in Fig. 1 and Table I. The ranges to be covered are the Heα plus Lyα spectra, 12.5–13.6 keV (time resolved); Heβ, 14.9–15.6 keV (time resolved); and Heα through Heβ range, 12.5–15.6 keV (time integrated).

II. SPECTROMETER GEOMETRY

The initial NIF instrument will be a compact spectrometer cassette mounted in a positioner diagnostic instrument manipulator (DIM) named dHIRES for "DIM High Resolution." A preliminary drawing of the instrument is shown in Fig. 2. The initial focus is the determination of electron density in compressed capsules from Stark broadening of the Heβ spectral lines of Kr, and inference of electron temperature from relative dielectronic satellite intensities. Spectra of both Heβ and Heα plus Lyα of Kr will be sagittally focused (direction perpendicular to the dispersion plane) onto different parts of the open slit of an x-ray streak camera using two conically bent crystals for time resolved measurements (30 ps). The Hall[2] conical design is used to provide a uniform sagittal focus along the streak camera photocathode, which is perpendicular to the spectrometer axis. The entire Heα plus Lyα through Heβ spectrum will be imaged by a cylindrical crystal, von Hamos spectrometer[3] onto an image plate (IP) on or near the source-to-detector axis, to provide a time integrated, calibration spectrum.

Note: Contributed paper, published as part of the Proceedings of the 21st Topical Conference on High-Temperature Plasma Diagnostics, Madison, Wisconsin, USA, June 2016.
[a)]Author to whom correspondence should be addressed. Electronic mail: khill@pppl.gov.

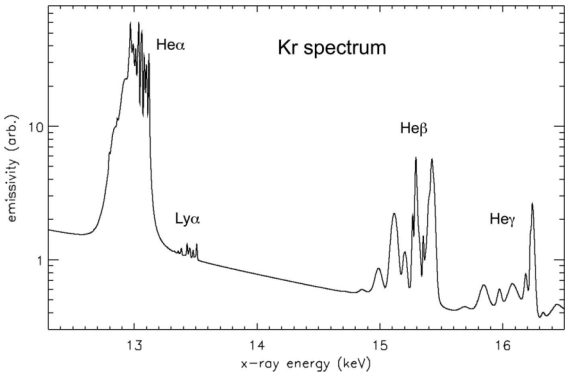

FIG. 1. Kr spectrum calculated by CRETIN[1] for $T_e = 4$ keV and $n_e = 5 \times 10^{24}$ cm^{-3}.

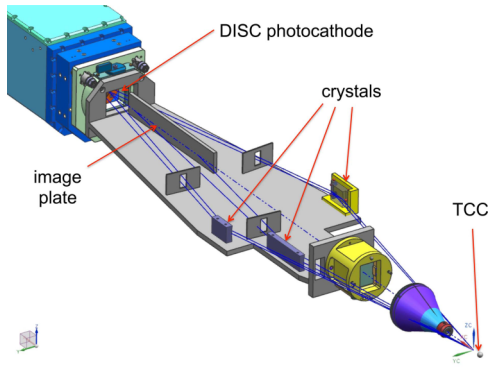

FIG. 2. Schematic illustration of the spectrometer cassette.

For deployment in the NIF polar DIM, the dimensions of the spectrometer cassette are tightly restricted by requirements to avoid the polar beam exclusion zone (38° with apex at 155.3 mm from target-chamber center (TCC)) yet to fit within the DIM diameter (~280 mm). Thus analytic ray-propagation calculations were done for the conical crystals in order to optimize the detector and crystal distances from the target-chamber center (TCC) and to study the spectral dispersion on the streak-camera (DISC) photocathode, as well as the sagittal focusing properties of the Hall conical crystal design. The crystal choices for the time resolved channels were driven by the desire to minimize the dispersion, dx/dE, due to the large spatial resolution elements (70-100 μm) of the DISC.[8]

The optimized design uses a conically bent Ge <220> crystal to provide high resolution measurements of the Kr Heβ spectrum and a conical quartz <11-10> crystal for the Kr Heα and Lyα spectral range. These spectra are diffracted onto the upper (Heα + Lyα) and lower (Heβ) parts of the 24-mm long DISC photocathode. A Si <111> crystal diffracts the full spectrum onto a single image plate within the spectrometer body and near the spectrometer axis. The spectral resolution of this time-integrated channel is not so critical, since its main function is to provide a relative calibration, using a single crystal, for the intensities of the two different Ge and quartz crystals. The restrictions for deployment in an equatorial DIM are much less strict than for the polar DIM.

III. EXPECTED PERFORMANCE

Photonics calculations using FLYCHK[4] and CRETIN and the estimated spectrometer solid angle of ~10^{-6} sr indicate that time resolution of order 30-100 ps can be obtained for 0.01 at. % Kr seeding in a D_2 capsule with $T_e = 4$ keV and $n_e = 5 \times 10^{24}$ cm^{-3}. NIF experiments using Kr-seeded symcaps are being done to evaluate Kr x-ray emission intensity from the lower resolution, broadband NIF X-ray Spectrometer (NXS) spectrometer.

TABLE I. Geometrical parameters, instrumental line broadening contributions, and solid angle for each of the three spectrometer channels.

Parameter	Units	Kr Heβ	Kr Heα and Lyα	Kr Heα – Heβ
Energy range	keV	14.9-15.6	12.8-13.6	12.8-15.6
Crystal (hkl)		Ge (220)	Quartz (110)	Si (111)
2d	Å	4.0004	4.9130	6.2708
Geometry		Conical	Conical	Cylindrical
Radius	mm	118	111	64
Crystal	mm	27	27	27
Length	mm	32	41	96
TCC to crystal	mm	580	580	460
TCC to detector	mm	1160	1160	920
Length on det.	mm	11.5	14.3	192
Det. resolution	μm	100	100	50
Detector		DISC	DISC	IP
Δθ rocking flat	μrad	41	9.3	26
ΔE flat	eV	1.54	0.31	1.29
ΔE with internal reflections	eV	1.56	1.75	3.84
ΔE source size 100 μm	eV	6.34	5.64	10.9
ΔE detector, 100 μm	eV	5.5	6.0	1.5
ΔE total	eV	8.5	8.4	11.6
E/ΔE		1600	1800	1200
Solid angle	μsr	1.4	1.7	3.5
Detector sensitivity		2%	2%	5.1 mPSL/ph

Estimates of the expected instrumental resolution and solid angle of the three spectrometer channels are summarized in Table I. The largest line broadening factors are source size and, for the DISC, the detector spatial resolution. Simulations showed factors of 5.6 and 3.2 broadening in the effective, flat crystal rocking curves for the quartz and silicon crystals, respectively, due to reflection from planes inside the crystal. These values are denoted "ΔE with internal reflections" in Table I. This broadening is negligible for the Ge crystal, since the x-rays penetrate only 21 μm in Ge, whereas the penetration depth is 480 μm in Si. This broadening occurs because an x-ray striking the crystal at a small Bragg angle will fall at different positions on the detector, depending on the depth inside the crystal at which the ray is effectively diffracted. These rays reflected from different depths are also reduced in intensity due to two path lengths (entering and exiting) of absorption by the crystal material. This broadening factor was determined by calculating the intensity of a single energy x-ray diffracted from many equally spaced planes inside the crystal at several Bragg angles across the rocking curve for that energy. The calculation was weighted by the reflectivity of the rocking curve at each Bragg angle and the transmission factor for the x-rays inside the crystal, and the resulting intensity at the detector was interpolated to a fixed detector spatial grid. The intensity of all these reflected rays was summed and normalized to the peak value of the rocking curve. The parameter "ΔE with internal reflections" is calculated from the full width at half maximum of this broadened and slightly shifted curve.

An additional broadening of the crystal rocking curve due to bending of the crystal is beyond the scope of this paper, since we do not have the calculation capability, but will be treated in a future publication in nuclear fusion. As an estimate of this broadening, Zastrau[5] calculated a factor of 32% increase in the rocking curve width at 8 keV, 33.5° Bragg angle, due to bending of a 60-μm thick GaAs <400> crystal to a cylindrical radius of 60 mm. The diffraction properties of GaAs are almost identical to those of Ge. We cannot directly apply this order of broadening to our crystals, since the broadening might vary with crystal planes, x-ray energy, and bending radius. These broadening factors, however, will be applied to the "ΔE with internal reflection" parameters, which are smaller than the ΔE values due to source-size. For example, a 32% increase in this value (3.84 eV) for the Si crystal leads to a total ΔE of 12.0, instead of 11.6. Also, this broadening factor decreases with increasing radius, so it is smaller for crystals bent to larger radius, such as the Ge and quartz crystals, than for those bent to smaller radius, such as the Si crystal. The IP detector sensitivity values are taken from Boutoux,[6] Table III, SR IP, and the spatial resolution from Seely.[7] DISC efficiencies and spatial resolution were taken from Opachich,[8] who quoted 4% efficiency for CsI photocathodes at 8 keV, and spatial resolution of 5–6.5 lp/mm for different streak cameras, or as small as 70 μm. We are assuming 100 μm for the present streak cameras, but an R&D program is in progress to improve the resolution.

IV. SUMMARY AND CONCLUSIONS

A spectrometer cassette to provide modestly high resolution measurements of the Heα, Heβ, and Lyα spectral regions of Kr is being designed for NIF to diagnose plasma conditions and mix in ignition capsules near stagnation times. Detailed design is beginning, and quotes for crystal fabrication have been received. The crystal quality will be tested in the Princeton Plasma Physics Laboratory (PPPL) x-ray laboratory, as will the alignment and calibration of the assembled spectrometer.

Design of the present spectrometer was complicated by the fact that the crystal should be midway between the source and the detector for both the Hall conical geometry and the von Hamos geometry. As the crystal is moved further from TCC to avoid the polar-beam exclusion zone, its distance from the axis must increase, since the largest Bragg angle is fixed. Thus, if moved too far, it interferes with the DIM walls. Also the Hall conical crystal geometry is known to be difficult to align, since neither the point-like source nor the detector is on the cone axis. Further, simulations indicate that only the inner 2 cm of the crystal width contributes to the sagittally focused image, thus limiting the maximum throughput. In order to resolve these difficulties, another imaging conical geometry is being developed,[9] hopefully to provide easier alignment, superior tolerance to misalignments, and higher throughput capability relative to the Hall geometry. In this new concept, the cone angle varies continuously to maintain the sagittal focus on the DISC photocathode at all energies, while the source always remains on the multi-cone axis. Also, a generalization of the von Hamos geometry, in which the cylindrical crystal is replaced by a simple conical crystal, allows one to place the crystal at arbitrary position between source and detector. If this geometry is developed, it could significantly alleviate the difficulties incurred in selection of crystals to optimize the spectral resolution within the constraints of the polar beam and DIM radius exclusion zones.

ACKNOWLEDGMENTS

This work was performed under the auspices of the U. S. DoE by LLNL under Contract No. DE-AC52-07NA27344 and PPPL under Contract No. DE-AC02-09CH11466.

[1]H. A. Scott, J. Quant. Spectrosc. Radiat. Transfer **71**, 689 (2001).
[2]T. A. Hall, J. Phys. E: Sci. Instrum. **17**, 110 (1984).
[3]L. von Hamos, Ann. Phys. **409**, 716 (1933).
[4]H.-K. Chung, M. H. Chen, W. L. Morgan, Y. Ralchenko, and R. W. Lee, High Energy Density Phys. **1**, 3 (2005).
[5]U. Zastrau, L. B. Fletcher, E. Foerster, E. Ch. Galtier, E. Gamboa *et al.*, Rev. Sci. Instrum. **85**, 093106 (2014).
[6]G. Boutoux, D. Batani, F. Burgy, J.-E. Ducret, P. Forestier-Colleoni *et al.*, Rev. Sci. Instrum. **87**, 043108 (2016).
[7]J. F. Seely, J. L. Glover, L. T. Hudson, Y. Ralchenko, A. Henins *et al.*, Rev. Sci. Instrum. **85**, 11D618 (2014).
[8]Y. P. Opachich, D. H. Kalantar, A. G. MacPhee, J. P. Holder, J. R. Kimbrough *et al.*, Rev. Sci. Instrum. **83**, 125105 (2012).
[9]M. Bitter *et al.*, Rev. Sci. Instrum. **87** 11E333 (2016).